06-8602/4

N00014-85-C-0206
NR 039-283 DATED 12/21/84

4

# MICROMECHANISMS OF FATIGUE CRACK GROWTH AND FRACTURE TOUGHNESS IN METAL MATRIX COMPOSITES

Technical Report for the Period 10/31/87 to 7/31/88

Prepared For

Office of Naval Research
800 North Quincy St.
Arlington, VA 22217

By D. L. Davidson

Southwest Research Institute
P. O. Box 28510
San Antonio, TX 78284



August 1988





SOUTHWEST RESEARCH INSTITUTE
SAN ANTONIO HOUSTON

# REPORT DOCUMENTATION PAGE

| | |
|---|---|
| 1a. REPORT SECURITY CLASSIFICATION<br>Unclassified | 1b. RESTRICTIVE MARKINGS |
| 2a. SECURITY CLASSIFICATION AUTHORITY | 3. DISTRIBUTION / AVAILABILITY OF REPORT<br>Unlimited |
| 2b. DECLASSIFICATION / DOWNGRADING SCHEDULE | |
| 4 PERFORMING ORGANIZATION REPORT NUMBER(S)<br>06-8602/4 | 5. MONITORING ORGANIZATION REPORT NUMBER(S)<br>4313283-02 |
| 6a. NAME OF PERFORMING ORGANIZATION<br>Southwest Research Institute<br>6b OFFICE SYMBOL (If applicable) | 7a. NAME OF MONITORING ORGANIZATION<br>Dr. Steven G. Fishman - Code 431N<br>Office of Naval Research |
| 6c. ADDRESS (City, State, and ZIP Code)<br>6220 Culebra Road<br>San Antonio, TX 78284 | 7b. ADDRESS (City, State, and ZIP Code)<br>800 North Quincy Street<br>Arlington, VA 22217-5000 |
| 8a. NAME OF FUNDING / SPONSORING ORGANIZATION<br>Office of Naval Research<br>8b. OFFICE SYMBOL (If applicable) | 9. PROCUREMENT INSTRUMENT IDENTIFICATION NUMBER<br>N00014-85-C-0206 |
| 8c. ADDRESS (City, State, and ZIP Code)<br>800 North Quincy Street<br>Arlington, VA 22217-5000 | 10. SOURCE OF FUNDING NUMBERS<br>PROGRAM ELEMENT NO. / PROJECT NO. / TASK NO. / WORK UNIT ACCESSION NO. |
| 11. TITLE (Include Security Classification)<br>Micromechanisms of Crack Growth and Fracture Toughness in Metal Matrix Composites<br>Fatigue | |
| 12. PERSONAL AUTHOR(S)<br>D. L. Davidson | |
| 13a. TYPE OF REPORT<br>Technical<br>13b. TIME COVERED<br>FROM 10/31/87 TO 7/31/88 | 14. DATE OF REPORT (Year, Month, Day)<br>August 1988<br>15. PAGE COUNT<br>27 |
| 16. SUPPLEMENTARY NOTATION | |

| 17. COSATI CODES | | |
|---|---|---|
| FIELD | GROUP | SUB-GROUP |
| | | |
| | | |

18. SUBJECT TERMS (Continue on reverse if necessary and identify by block number)
KEY WORDS: Metal matrix composites, silicon carbide reinforcement, fatigue crack growth, fracture toughness, particulate strengthening, crack growth micromechanisms.

19. ABSTRACT (Continue on reverse if necessary and identify by block number)

Fatigue crack rate data for large cracks in 12 variations of particulate Silicon Carbide SiC reinforced alloy composites have been measured. Composites with seven different matrix alloys were tested, four of which were of precipitation hardening compositions, and these were tested in both as-extruded and peak aged conditions. Five of the materials were made by casting, ingot metallurgical methods and two of the alloys by mechanical alloying, powder metallurgical methods. For both manufacturing methods, primary fabrication was followed by hot extrusion.

The fatigue crack growth curves exhibited a linear, or Paris law region, fitting the function $da/dN = B\Delta K^s$, and a threshold stress intensity factor. As has been found for other materials, the coefficients B and S are correlated; for these materials lnB-116.4-2.1s. A correlation was also found between $\Delta K_{th}$ and s, and it was found possible to compute the magnitude of $\Delta K_{th}$ using a simple model for the threshold together with yield stress and SiC size and volume fraction. The results obtained were explained using the relationship between $\Delta K_{th}$ and crack closure determined previously for unreinforced aluminum alloys. Fatigue

| | |
|---|---|
| 20. DISTRIBUTION / AVAILABILITY OF ABSTRACT<br>☐ UNCLASSIFIED/UNLIMITED ☒ SAME AS RPT. ☐ DTIC USERS | 21. ABSTRACT SECURITY CLASSIFICATION<br>Unclassified |
| 22a. NAME OF RESPONSIBLE INDIVIDUAL<br>David L. Davidson | 22b. TELEPHONE (Include Area Code) 512/522-2314<br>22c. OFFICE SYMBOL |

DD FORM 1473, 84 MAR — 83 APR edition may be used until exhausted. All other editions are obsolete.

19. crack growth is through the matrix for these composites, and the SiC has the effect of altering the slip distance, therefore, the plasticity accompanying fatigue cracks. It was shown that all the crack growth rate curves were reduced to one equation having the form $da/dN=B'\Delta K_{eff}^{s'}$, where $B'=6.5\times10^{-9}$ m/cy and $s'=1.7$. A partly theoritical method for predicting fatigue crack growth rates for untested composites is given.

TABLE OF CONTENTS

# THE GROWTH OF FATIGUE CRACKS THROUGH PARTICULATE SiC REINFORCED ALUMINUM ALLOYS

D. L. Davidson
Southwest Research Institute
San Antonio, Texas 78284

## INTRODUCTION

Aluminum alloys may be made lighter and stiffer by the addition of silicon carbide [1]. With the use of particulate SiC as reinforcement, composites of approximately isotropic directional properties may be made. Three approaches to the blending of constituants have been used: (1) the mixing of SiCp into molten aluminum, followed by casting; (2) mechanical joining, or alloying, of the two constituants by high-energy attrition; and (3) the mechanical mixing of aluminum alloy powders and SiCp. The last two approaches result in powders, which require that the techniques of powder metallurgy be used to consolidate the composite. Since a nearly isotropic product is desirable, it is necessary to obtain a good dispersion of SiCp using these processes.

The advantages of SiCp additions to aluminum alloys are countered by the observation that these composites have lowered fracture toughnesses than the aluminum alloys used as matrix materials. It is not known if this is an intrinsic property of these composites, or if methods of increasing the fracture toughness to more acceptable levels may be devised. The fatigue crack growth rate characteristics have also been found to be different for the composites than for the base aluminum alloys.

The principal variables associated with these composites are: (1) the size, (2) size distribution and (3) the volume fraction of SiCp, and the (4) composition and (5) heat treatment of the matrix aluminum alloy. Of course, the strength of the interface could be the most important factor governing the fracture characteristics of the material, but for most commercially available composites, the interface is stronger than the matrix, and is not a variable. There are also many variables related to the fabrication of the composite into final product form. Each of these variables potentially could control the mechanical properties of the composite; therefore, a systematic variation of each quantity would be the ideal method of optimizing the properties of the composite. However, due to the limitations imposed by processing, such a

systematic variation has not been undertaken. Rather, the more feasible approach is to purchase composites from manufacturers who have determined the optimum processing conditions for a particular manufacturing method. The physical and mechanical properties of each material are then characterized. This paper reports on the fatigue properties of these composites.

## MATERIALS

In the research reported here, the emphasis has been on determining the fatigue crack growth characteristics for composites manufactured by the first two methods described above. With the cast material, a relatively low-cost product on which little research has been reported, it was possible to obtain composites having different aluminum alloys as the matrix, but with SiCp of only one size and size distribution. To obtain smaller sized SiCp, two mechanically alloyed composites were obtained, but great variation in matrix alloy composition was not possible. Supplier of the cast material was Dural Aluminum Composite Company of San Diego, California, and supplier of the mechanically joined material was Novamet, a division of International Nickel Company, now located in Huntington, West Virginia. The exact date of manufacture of these composites is unknown, but it was sometime during 1985 for the mechanically alloyed material and early 1986 for the cast material.

The materials tested are listed in Table 1. All composites were received (AR) in the extruded condition as bars about 1 m long having a rectangular cross section approximately 12 x 100 mm. Extrusion ratios are unknown. Specimen blanks were cut from the bars and half those capable of precipitation strengthening were heat treated to the peak aged condition (PA) according to the manufacturer's recommendations.

Tensile stress-strain experiments have been performed on some of the composites. Likewise, particle contents have been carefully characterized for some of the composites, but not all. Particle characterization is a difficult process because of the great size range found in these materials, particularly those manufactured by mechanically alloying. Image processing of photographs ranging from 200 to 22,000 magnification was required for alloy 1 [2]. A second method was used to examine only the SiC particulate of some of the other alloys. For this second method, the SiC must be separated from the matrix alloy by digesting with mixed acids. Then the particle size and volume fraction are determined by a sedimentary, x-ray technique. The sizes and size

distributions determined by this method were in approximate agreement with those determined for larger particles by image processing, and for the cast materials, were approximately the same for the two alloys sampled. Because of problems associated with separating particles from matrix, smaller particles are not measured by the latter technique.

## EXPERIMENTAL

Fatigue cracks were initiated from the tip of a 23 mm deep notch in a compact tension specimen approximately 62 mm on each side by 6.5 mm thick made so that the crack would grow perpendicular to the extrusion direction. This specimen was cycled in a servohydraulic, computer controlled fatigue machine at 10 Hz, and the crack length was monitored with a clip gauge attached to the notch mouth. The fatigue crack was initiated at approximately $\Delta K = 6$ MPa$\sqrt{m}$, $R = 0.1$, then down loaded under computer control, using methods described in ASTM E647, to determine the approximate threshold cyclic stress intensity factor, $\Delta Kth$, for fatigue crack growth. Load was then increased, and the crack growth rate was measured as $\Delta K$ increased with lengthening of the crack. Fracture toughness was measured at the point of fast fracture; data on this property has been reported and analyzed elsewhere [3].

Fatigue crack growth results for several alloys were satisfactorily duplicated, using other equipment. Both a large compact tension specimen and a single edge notch specimen were used in conjunction with a traveling microscope for monitoring crack length.

Fractographic examination was made of broken specimens using the scanning electron microscope. Two values of $\Delta K$ were chosen for this examination, one near $\Delta Kth$ and the other just before the transition to fast fracture.

## RESULTS

Fatigue crack growth rates for selected alloys are shown in Figs. 1 - 4. These figures, which are typical of all those measured, compare (1) the effect of 15 vs 25 v/o SiC in a matrix of 2014 alloy in the as received condition and (2) the effect of heat treating to peak age for a matrix of 7475 alloy with 15 v/o SiC. Each material is seen to exhibit a linear, Stage II (Paris) region fitting the function:

$$da/dN = B\Delta K^s \qquad (1)$$

Values of the coefficients B and s derived for each of the materials are listed in Table 1, together with the values of $\Delta K_{th}$ measured.

Table 1
Fatigue Crack Growth Parameters - This work

| Comp. No. | Designation (+ __v/o SiC) | Condition | B (m/cy) | s | $\Delta K_{th}$ (MPa$\sqrt{m}$) |
|---|---|---|---|---|---|
| 1 | IN-9052 +15 | AR | $1.1\times10^{-12}$ | 6.0 | 4.1 |
| 2 | Al-4Mg +15 | AR | $6.1\times10^{-13}$ | 5.7 | 3.3 |
| 3 | IN-9021+14 | AR | $1.1\times10^{-12}$ | 5.2 | 3.3 |
| 4 | IN-9021+14 | PA | $2.1\times10^{-11}$ | 4.2 | 3.6 |
| 5 | 2014 +15 | AR | $2.1\times10^{-12}$ | 4.6 | 3.6 |
| 6 | 2014 +15 | PA | $9.2\times10^{-12}$ | 4.4 | 4.3 |
| 7 | 2014 + 25 | AR | $4.1\times10^{-13}$ | 5.4 | 4.7 |
| 8 | 2014 + 25 | PA | $8.1\times10^{-13}$ | 5.3 | 4.3 |
| 9 | 2024 +15 | PA | $8.3\times10^{-13}$ | 4.7 | 4.4 |
| 10 | 2024 - T351* | PA | $4.0\times10^{-11}$ | 4.0 | 3.5 |
| 11 | 7475 +15 | AR | $3.0\times10^{-12}$ | 4.6 | 3.5 |
| 12 | 7475 +15 | PA | $8.3\times10^{-12}$ | 5.1 | 4.7 |

*Matrix material without SiC. AR = As Received PA = Peak Aged

In addition to these data, similar information exists in the literature for other alloys and composites. Data appropriate to the current work has been summarized in Table 2.

Table 2
Fatigue Crack Growth Parameters - Others

| Comp. No. | Designation (+ __v/o SiC) | Condition | B (m/cy) | s | $\Delta K_{th}$ (MPa$\sqrt{m}$) | Source |
|---|---|---|---|---|---|---|
| 13 | 6061 + 25 | F | $5.7 \times 10^{-16}$ | 8.1 | 4.7 | [4] |
| 14 | 6061 + 25 | T6 | $1.3 \times 10^{-13}$ | 6.5 | | [4] |
| 15 | 2124 | UA | $4.0 \times 10^{-10}$ | 2 | 1 | [5] |
| 16 | 2124 +13* | UA | $2.9 \times 10^{-11}$ | 3 | 2.2 | [5] |
| 17 | 2124 | OA | $4.0 \times 10^{-10}$ | 2 | 1.5 | [5] |
| 18 | 2124 +13* | OA | $2.6 \times 10^{-12}$ | 3.3 | 3.3 | [5] |
| 19 | MB 78 | T6 | $1.8 \times 10^{-14}$ | 7.8 | 4.2 | [6] |
| 20 | MB78 + 20Cp | T6 | $2.9 \times 10^{-12}$ | 5.1 | 4.2 | [6] |
| 21 | MB78 + 20Fp | T6 | $2.8 \times 10^{-11}$ | 3.6 | 3.0 | [6] |
| 22 | IN 9052 | F | $1.3 \times 10^{-9}$ | 2.4 | 2.0 | [7] |
| 23 | IN 9021 | T4 | $3.1 \times 10^{-10}$ | 2.7 | 2.5 | [7] |

*SiC whisker reinforced  Cp = Coarse particles  Fp = Fine Particles

The data of Christman and Suresh [5] was included in Table 2 even though it was on whisker reinforced material because of the accurate determination of $\Delta K_{th}$ made by compression-compression testing.

The data in Tables 1 and 2 were examined for a correlation between the constants B and s in eq. (1). The result is shown in Fig. 5, which gives the relation

$$\ln B = -16.1 - 2.2s \qquad (2)$$

Correlations between these two coefficients have been made by many investigators [8], but eq. (2) differs from that found for steels, which is $\ln B = -14.3 - 3.83s$. An even greater difference exists between eq. (1) and the results of Bailon, et al. [9], for aluminum alloys. Their results were found to be stongly R dependent, but for R = 0.1 gave $\ln B = -0.143 - 0.375s$. The reason for this large difference is unknown. The line for steels is shown on the figure for

comparison to present results.

Equation (2) may more conveniently be written as

$$s = - 7.32 - 0.455 \ln B \qquad (3)$$

This correlation shows that B and s for composites are part of the family of curves which exist for unreinforced aluminum alloys, as opposed to any parallel shifts which might have existed in these crack growth curves.

The data in Table 1 show values of $\Delta K_{th}$ for composites which are larger than generally found for the matrix alloys alone, a condition also found by Logsdon and Liaw [4] and by Christman and Suresh [5], but not by Shang and Ritchie [6].

To examine the changes in $\Delta K_{th}$, a previously developed concept of the origin of the threshold has been invoked [10,11]. That concept was derived from the observation that Mode II opening composed a large proportion of the crack opening displacement for cracks growing near $\Delta K_{th}$ [12]. Thus, the threshold was conceived of as being a crack tip from which a single slip band emanates ahead of the tip, therefore, in Mode II. The Mode I stress intensity factor for this geometry is

$$\Delta K_{th} = \sigma_f \sqrt{2\pi r_s} \qquad (4)$$

where $\sigma_f$ = the flow stress of the material at the end of the slip band, and $r_s$ = length of the slip band. For the two aluminum alloys 7075 and 7091, the mean free path of dislocation motion through the dispersoids was identified as being the microstructural factor controlling fatigue crack growth rate, and by inference, the magnitude of $\Delta K_{th}$ [13].

For particulate reinforced composites, the volume fraction, $v_f$, and particle size, d, of SiC particles may be combined to compute a mean free path for slip from the relation [14]:

$$r_s = (2d/3)(1-v_f)/v_f \qquad (5)$$

This computation of a mean free path is complicated by the size distribution of

This computation of a mean free path is complicated by the size distribution of particles within these materials, so only "the most probable value of particle size," which is the peak of the distribution curve, has been used in the calculation.

The necessary information for computation of mean free path is not available for all of the materials in either Table 1 or 2, and the appropriate value of $\sigma_f$, which is probably the stress at proportional limit, is also not generally available. Therefore, $\sigma_f$ = yield stress, defined at 0.2% offset strain, has been used. The data used and the values of $\Delta K_{th}$ calculated are listed in Table 3.

Table 3
Computation of $\Delta K_{th}$

| Mater. No. | Designation (+ _v/o SiC) | Condition | $V_f$ | d (μm) | $\sigma_y$ MPa | $\Delta K_{th}$(comp) ------- MPa√m | ΔKth(meas) -------- |
|---|---|---|---|---|---|---|---|
| 1 | IN 9052 + 15 | AR | .17 | 9 | 450 | 5.3 | 4.1 |
| 6 | 2014 + 15 | PA | .15 | 15 | 319 | 4.9 | 4.3 |
| 12 | 7475 + 15 | PA | .16 | 14 | 300 | 4.2 | 4.4 |
| 20 | MB 78 + 20Cp | PA | .225 | 10 | 500 | 6.0 | 4.2 |
| 21 | MB 78 + 20Fp | PA | .21 | 6 | 400 | 3.9 | 3.0 |

The calculated and measured values of $\Delta K_{th}$ are compared in Fig. 6, where it is seen that $\Delta K_{th}$(calc) is consistantly larger than $\Delta K_{th}$(meas) by a factor of about 1.18; therefore,

$$\Delta K_{th}(\text{meas}) = 0.85\Delta K_{th}(\text{calc}) \qquad (6)$$

The accuracy of the computed threshold values might be improved by using the proportional limit for $\sigma_f$, but also a more realistic use of the size distribution function should be sought.

There is correlation between measured values of $\Delta K_{th}$ and the fatigue coefficient s, as is shown in Fig. 7, which yields the relation

$$s = 1.18\Delta K_{th}(meas) \quad (7)$$

Combining eqs. (6) and (7) gives

$$s = \Delta K_{th}(calc) \quad (8)$$

Underlying causes for the simplicity of this expression have been sought from the physics of the crack growth process, but an explanation has yet to be found.

## DISCUSSION

Fatigue crack growth curves in particulate reinforced aluminum composites exhibit a systematic variation in Paris law parameters similar to those observed in steels [8] and other aluminum alloys [9]. This correlation can be readily understood (1) because the dominant fracture mode is crack growth through the matrix, and (2) by examining the relation between the Paris law parameters and $\Delta K_{th}$. Since failure is mainly through the matrix, the Paris law parameters would be expected to have some relationship to those for the unreinforced alloys.

Also, it appears that $\Delta K_{th}$ is related to yield stress and the SiC particle size and volume fraction through the Mean Free Path, which is interpreted as being the average slip distance for dislocations moving through the composite. Since scatter exists in this correlation, and there are only 5 data points, this concept should be regarded presently as a hypothesis, and needs further testing. Furthermore, describing these composites with a single "mean free path" is to greatly simplify a very complex microstructure. Dislocations actually interact with a distribution of particle sizes with different volume fractions, and perhaps different characteristics. Better ways of accounting for the complexities of the particle distribution are badly needed to further refine this concept of $\Delta K_{th}$. However, this is a logical mechanism for the threshold, and even in its present, rudimentary state, it does provide a method for understanding and systemitizing the effects of SiC particle additions.

The good correlation between $\Delta K_{th}$ and s, the slope of the crack growth rate curve, is easily understood as the effect of fatigue crack closure through the

function derived for other materials [15]

$$\Delta K_{eff} = \Delta K - \Delta K_{th} \qquad (9)$$

which implies that materials with a higher $\Delta K_{th}$ should have more closure. The behavior represented by eq. (9) has been observed quantitatively for the aluminum alloys 7075 and 7091 and 304 stainless steel using crack closure measurements by stereoimaging [15], and qualitatively by Shang and Ritchie [6] using a far-field closure technique. The effect of increasing Mean Free Path is to increase $\Delta K_{th}$ because of the increase in slip distance of dislocations, with the corresponding increase in crack tip plastic zone size. When ΔKth is increased, the slope of the da/dN - ΔK curve also increases, providing that there is a point on that curve at high ΔK which is largely unaffected by closure. As may be seen in the correlation between Paris law coefficients, this "rotation" of da/dN - ΔK curves is occuring.

Also, it should be noted that eq. (4) implies that plasticity is responsible for $\Delta K_{th}$, and that it is the compressive residual stresses ahead of the crack tip caused by this plasticity which sets the level of the threshold. Therefore, $\Delta K_{th}$ is the manifestation of plasticity induced crack closure. Crack wake plasticity effects are likely to have a minimal influence on $\Delta K_{th}$ because of the largely Mode II opening for cracks at threshold. Of course, there are other mechanisms which could influence crack closure, and a plethora of them have been conceived [16]. One of these mechanisms which has been demonstrated to have considerable influence is oxide wedging[17], and since these fatigue crack growth experiments were conducted in an environment of about 50% relative humidity, this mechanism may be the cause of some of the scatter in the correlations, and would have the most influence on $\Delta K_{th}$.

A number of other investigators have suggested that a length parameter could be used in a relation similar to eq. (4) for defining $\Delta K_{th}$, but it has been difficult to define this parameter. Some of the parameters suggested have been a "microstructural parameter [18]," plastic zone size [19,20], and the grain diameter [19,21]. For certain titanium alloys [21] and some steels [19], grain size and yield stress have correlated satisfactorily with $\Delta K_{th}$ through a relation similar to eq. (4).

A three parameter definition of ΔKth ($\sigma_f$, d and $V_f$) is more reasonable than in terms of yield stress alone, as was demonstrated by Ritchie and Knott for steels [22], and for these SiCp reinforced aluminum alloys composites, the microstructural parameter has been reasonably well defined, given the limitations of handling particle size distributions. For unreinforced matrix alloys, the mean free path for dislocation motion at threshold is apparently regulated by dispersoids [13], which seem to exist in about the same size range and volume fraction for all commercial aluminum alloys [23]. This would make MFP about the same for all aluminum alloys, and is one explanation for why fatigue crack growth rate curves and ΔKth values for all aluminum alloys lie in such a narrow range (excluding environmental effects). Whether or not dispersoids in the base alloys for these composites are similar to those found in unreinforced alloys has not been adequately explored.

The correlation found between the fatigue exponent s and ΔKth, eq. (7), is qualitatively similar to that found for steels by Tanaka [24], and when interpreted as the effect of crack closure, these relationships are reasonable and to be expected.

## IMPLICATIONS FOR PREDICTING FATIGUE BEHAVIOR OF COMPOSITES

The correlations found through this research should make it possible to derive the crack growth behavior for large fatigue cracks in composites knowing only the flow stress and the characteristics of the SiC particulate. Summarized below is the sequence for deriving fatigue crack growth rates:

1. Compute the MFP using eq. (5),
2. Compute ΔKth(calc) using eq. (4),
3. Determine s from eq. (8),
4. Compute B using eq. (2) or (3),
5. Insert B and s into eq. (1) to determine crack growth rates.

An example of this proceedure is shown in Fig. 8, where s values were varied between 2 and 7. Since the complete fatigue crack growth characteristics are known, it is then possible to convert this family of curves to one curve using the modified Paris law relation

$$da/dN = B'\Delta K_{eff}^{s'} \qquad (10)$$

where ΔKeff was defined in eq. (9). The best values derived are:

$$B' = 6.5 \times 10^{-9} \pm .5 \times 10^{-9} \text{ m/cy, and}$$

$$s' = 1.7 \pm .3 \qquad (11)$$

Ideally, all the curves would reduce to one value of B' and s' if all the governing equations were correct, and this would provide a check on the equations empirically derived. The sensitivity of B' and s' to the magnitudes of the constants in the governing equations was extensively tested, and the values given in eq. (11) minimize variations for $2 < s < 6$. The derived values of B' and s' were found to be very sensitive to the constants in eq. (2) and (8). The values of the constants used to derive eq. (11) were:

$$\ln B = -16.4 - 2.1s \quad \text{and} \quad \Delta K_{th} = 0.82s$$

The constants in these equations are somewhat different than those derived from the experimental data. However, they are not sufficiently different to indicate an error in interpretation. The main variations in computed B' and s' occur at the extreme values, indicating that eq. (2) may not be very accurate for $s < 2$ or $s > 6$.

## CLOSURE

The results of this work indicate that fatigue crack growth characteristics for SiCp reinforced composites are similar to those of the matrix aluminum alloys. The key to this result is the correlation found between B and s in the Paris law, together with the correlation between s and the computed $\Delta K_{th}$ derived from size and volume fraction of the SiCp. This latter approximation is a simplification of the complex effects of a distribution of large particles and must be so considered. Therefore, the results of tests on a specific composite may not yield results which are completely compatible with the framework developed here, particularly for extremes in the Paris equation exponent s. These research results do, however, provide a systematic and logical rationalization to fatigue crack growth through this class of materials, even though the details of fatigue crack growth are still being explored.

## CONCLUSIONS

1. Fatigue crack growth rate curves for SiCp reinforced aluminum alloy composites are generally similar to those of the matrix alloys. This is because the crack was found to grow mainly through the matrix.

2. A correlation was found between the crack growth rate coefficient (B) and exponent (s) in the Paris equation. Similar correlations have been found also for steels.

3. The Paris law exponent s correlates with $\Delta K_{th}$ for the composites and unreinforced matrix alloys, with the result that $s = 0.82\Delta K_{th}$.

4. It is possible to compute an approximate $\Delta K_{th}$, using yield stress and SiCp size and volume fraction, which correlates reasonably well with measured values, although the data for this correlation are limited.

5. Using the previously developed concept that fatigue crack closure is a manifestation of the threshold, so that $\Delta K_{eff} = \Delta K - \Delta K_{th}$, all the composite data may be reduced to $da/dN = B'\Delta K_{eff}^{s'}$, where B' and s' values are approximately the same for all composites.

## ACKNOWLEDGEMENTS

The author is grateful to The Office of Naval Research, Contract N00014-85-C-0206, Dr. S.G. Fishman, contract monitor, for supporting this research, and to John Campbell and James Spencer for proficiently performing many of the measurements.

## REFERENCES


1. A.P. Divecha, S.G. Fishman, and S. D. Karmarker, *J. Metals* **33**, 12 (1981).
2. D.L. Davidson, *Met. Trans. A.* **18A**, 2115 (1987).
3. D.L. Davidson, *J. Mat. Science*, in press (1988).
4. W.A. Logsdon and P.K. Liaw, *Engng. Fract. Mech.* **24**, 737 (1986).
5. T. Christman and S. Suresh, *Mat. Sci. and Engng.*, in press (1988).
6. J. Shang and R.O. Ritchie, *Mat. Sci. and Engng.*, in press (1988).
7. D.L. Erich and S.J. Donachie, *Metals Progress* **122**, 22-25 (Feb. 1982).
8. M.B. Cortie and G.G. Garrett, *Engng. Fract. Mech.* **30**, 49 (1988).
9. J-P. Bailon, J. Masounave and C. Bathias, *Scripta Metallurgica* 11 1101-1106 (1977).
10. D.L. Davidson, *Acta Metallurgica* **22**, 707-714 (1984).
11. D.L. Davidson, *Acta Metallurgica* **26**, in press (1988).
12. D.L.Davidson and J. Lankford, *Mat. Science and Engng.* **60**, 225-229 (1983).
13. D.L.Davidson and J. Lankford, *Mat. Science and Engng.* **74**, 189-199 (1985).
14. J.W. Martin, *Micromechanisms in Particle-hardened Alloys* Cambridge University Press, 1980, p. 43.
15. S.J. Hudak and D.L. Davidson in *Mechanics of Fatigue Crack Closure*, J.C. Newman and W. Elber, eds., ASTM STP 982, ASTM, 1988, pp. 121-138.
16. S. Suresh and R.O. Ritchie in *Fatigue Crack Growth Threshold Concepts*, D.L. Davidson and S. Suresh, eds. The Metallurgical Society- AIME, 1984, pp. 227-261.
17. A.K. Vasudevan and S. Suresh, *Met. Trans. A.* **13A**, 2271 (1982).
18. G.M. Lin and M.E. Fine, *Scripta Met.* **16**, 1249-1254 (1982).
19. D. Taylor in *Fatigue Thresholds, v. 1*, J. Backlund, A.F. Blom and C.J. Beevers, eds, EMAS, Cradley Heath, UK, 1982, pp. 455-470.
20. Y. Chonghua and Y. Minggao, *Fat. of Eng. Mat. and Struct.* **3**, 189-192 (1980).
21. G.R. Yoder, L.A. Cooley and T.W. Crooker, *Engng. Fract. Mech.* **11** 805-816 (1979).
22. R.O. Ritchie and J.F. Knott, *Acta Metallurgica* **26**, 147 (1973).
23. W.G. Truckner, J.T. Staley, R.J. Bucci and A.B. Thakker, Tech. Rep. AFML-TR-76-169 (Air Force Materials Laboratory, Wright-Patterson Air Force Base, OH), 1976, p. 24.
24. K. Tanaka, *International J. of Fracture* **15**, 57-68 (1979).

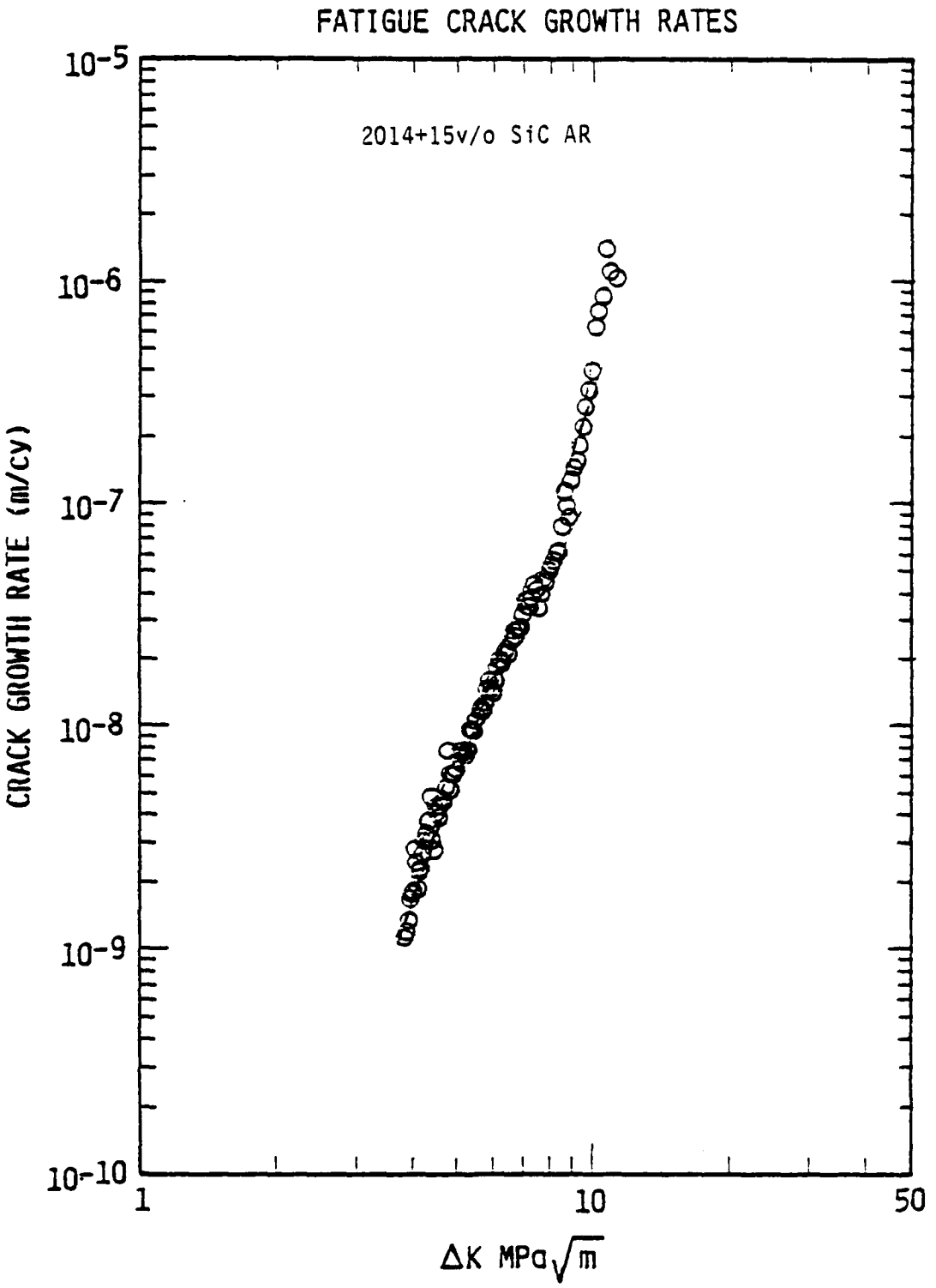


Fig. 1 Fatigue crack growth rate curve for 2014 + 15v/o SiCp composite as received at R = 0.1, 10 Hz, laboratory air.

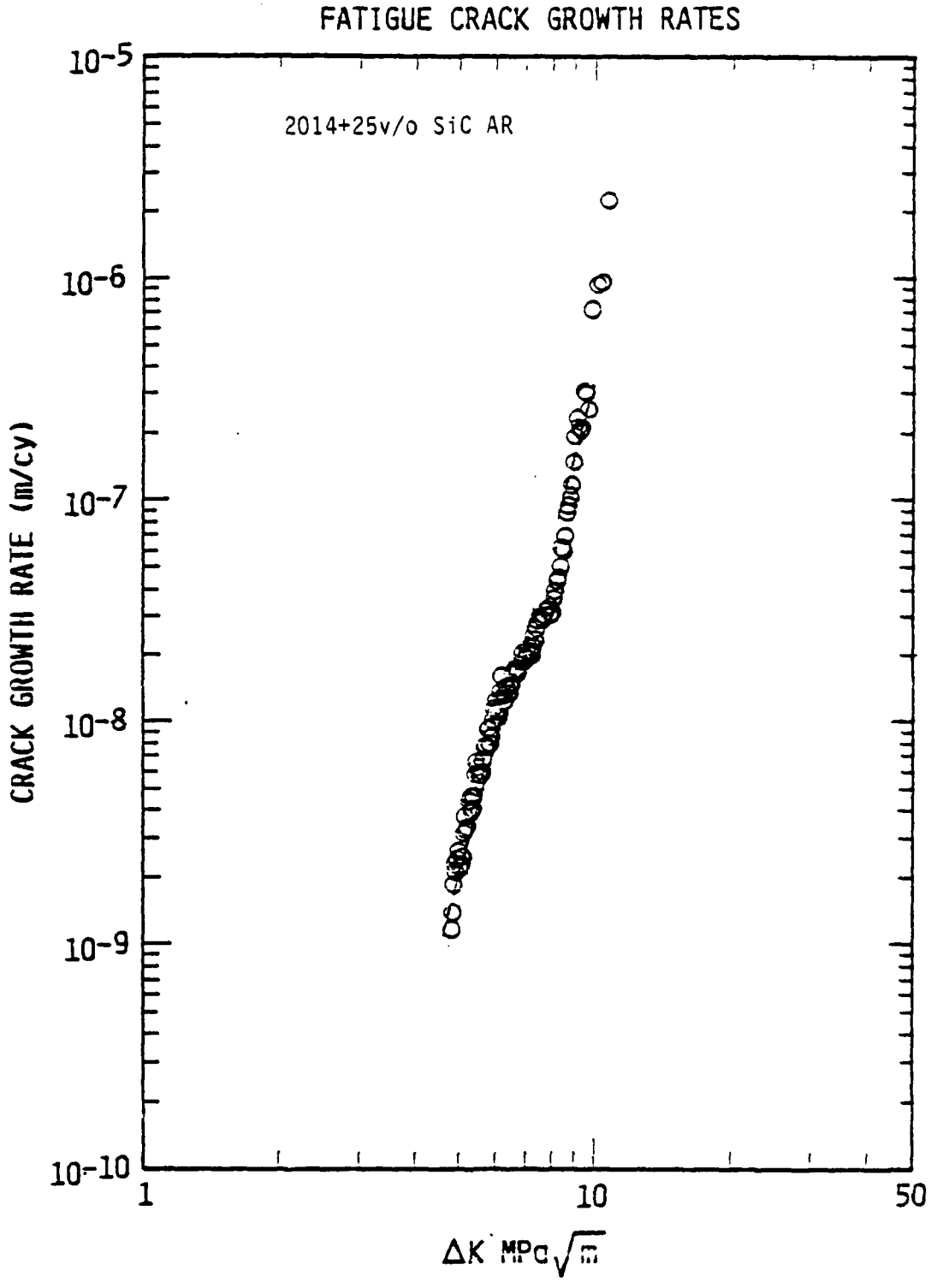


Fig. 2 Fatigue crack growth rate curve for 2014 + 25v/o SiCp composite as received at R = 0.1, 10 Hz, laboratory air.

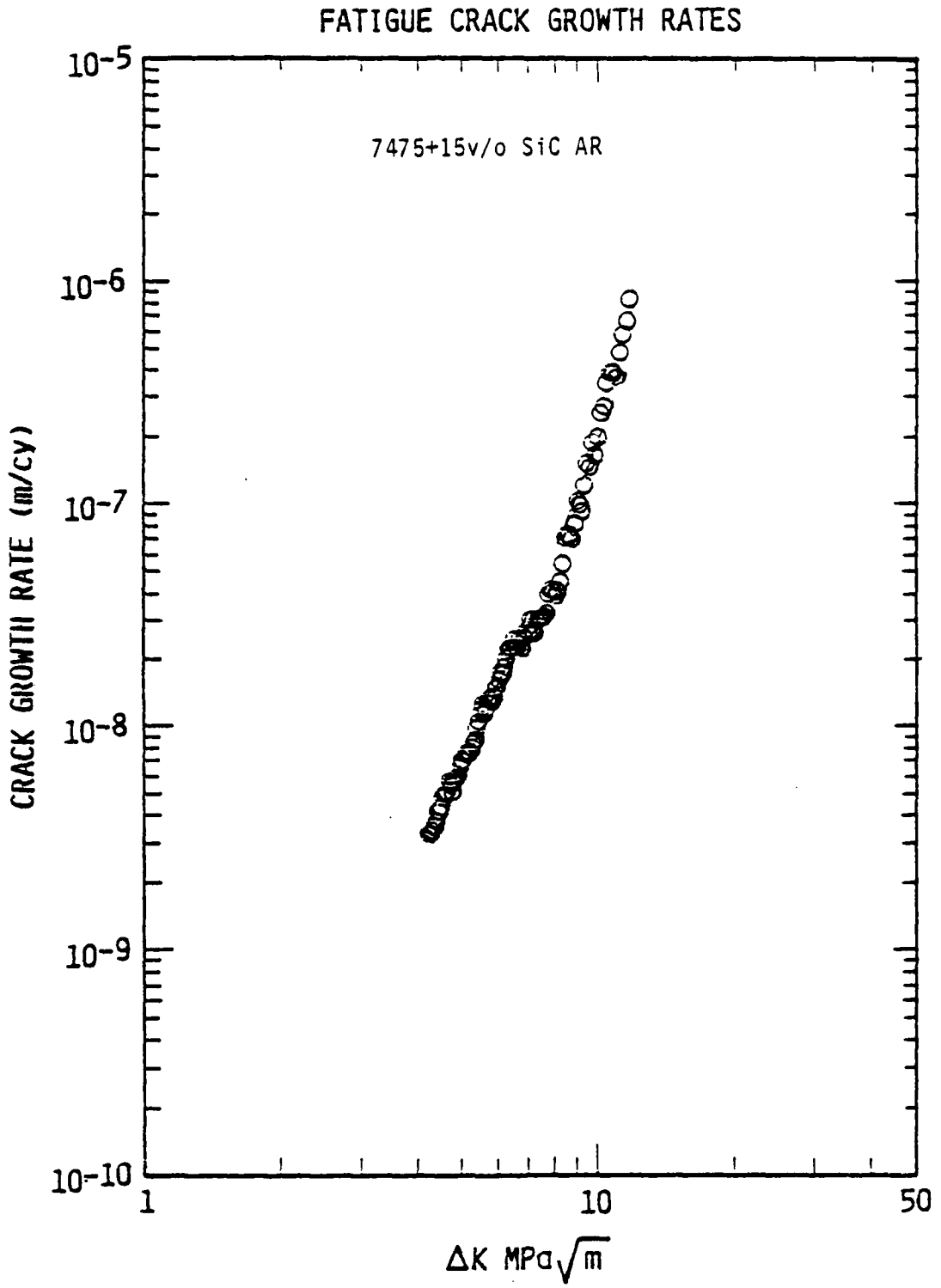


Fig. 3 Fatigue crack growth rate curve for 7475 + 15v/o SiCp composite as received at R = 0.1, 10 Hz, laboratory air.

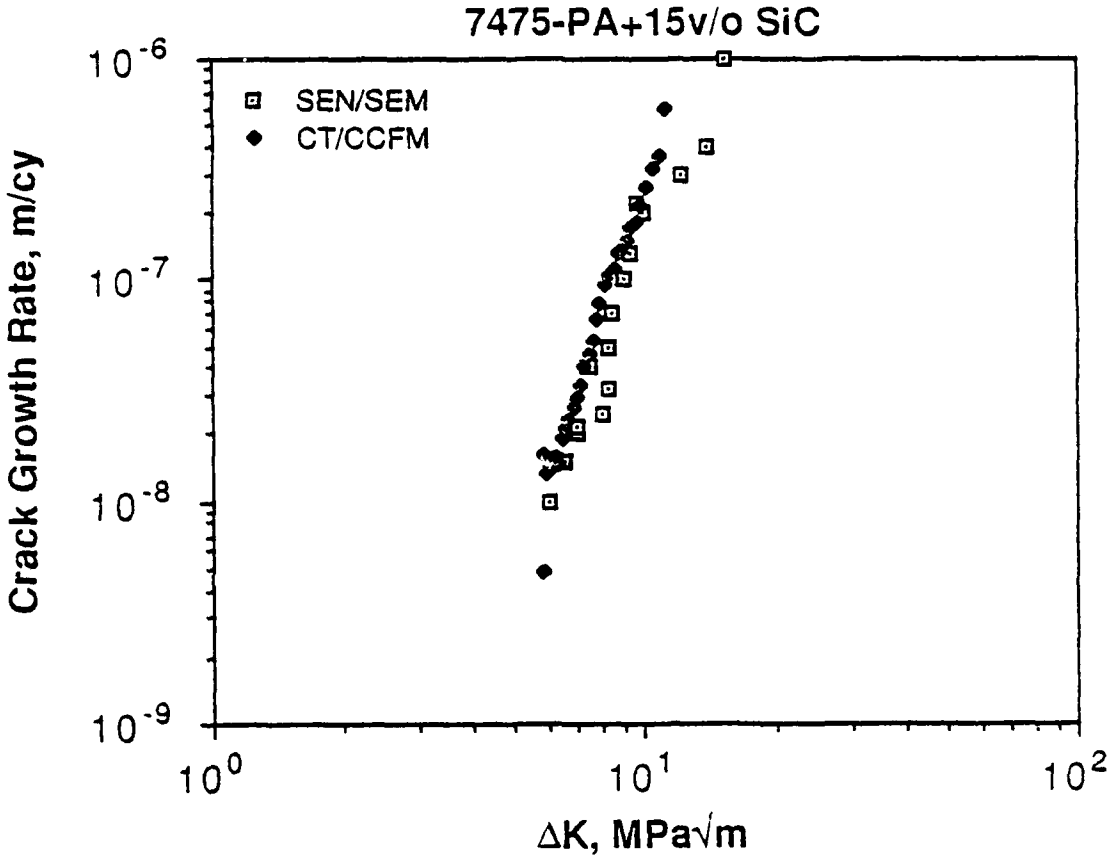


Fig. 4 Fatigue crack growth rate curve for 7475 + 15v/o SiCp composite peak aged at R = 0.1, 10 Hz, laboratory air. Also shown is the approximate agreement between data obtained from the computer controlled machine using a CT specimen and using a microscope to measure crack length from a SEN specimen.

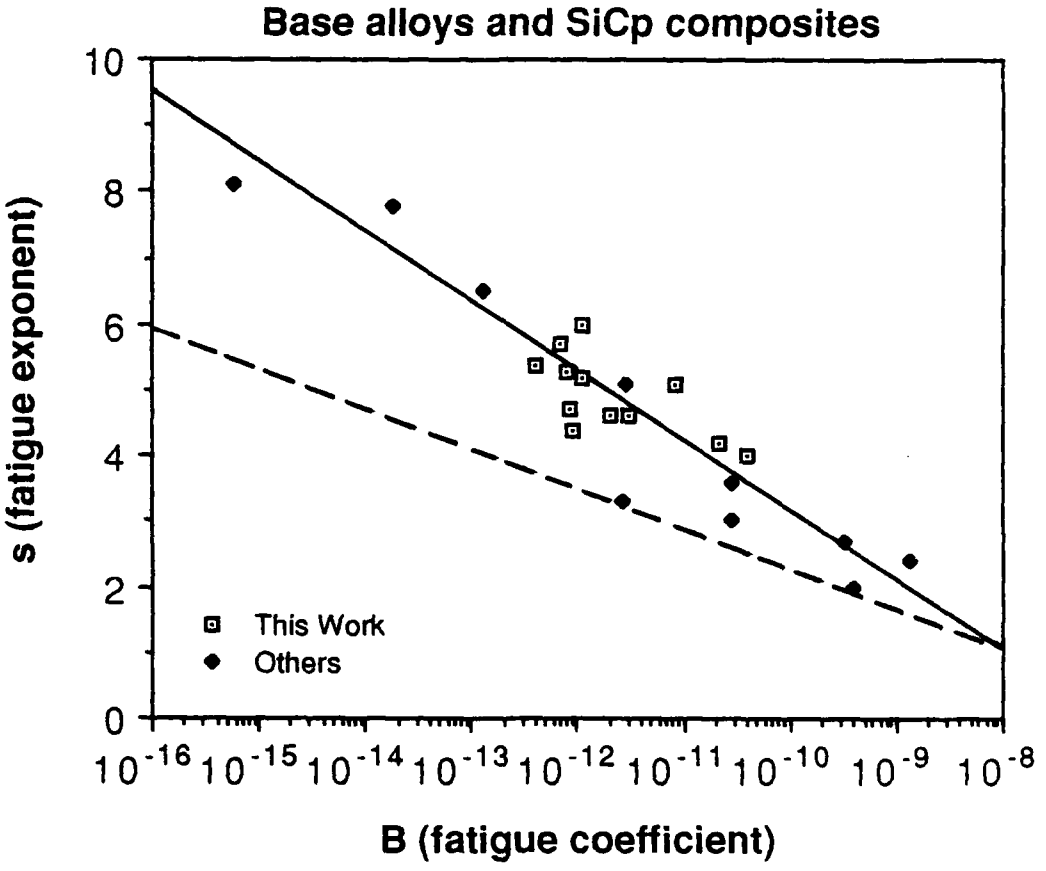


Fig. 5 Correlation between coefficients in the Paris law for the materials studied here (Table 1) with data obtained from others (Table 2). The dashed line, for comparison, is the correlation found by Tanaka for steels, as quoted in [8].

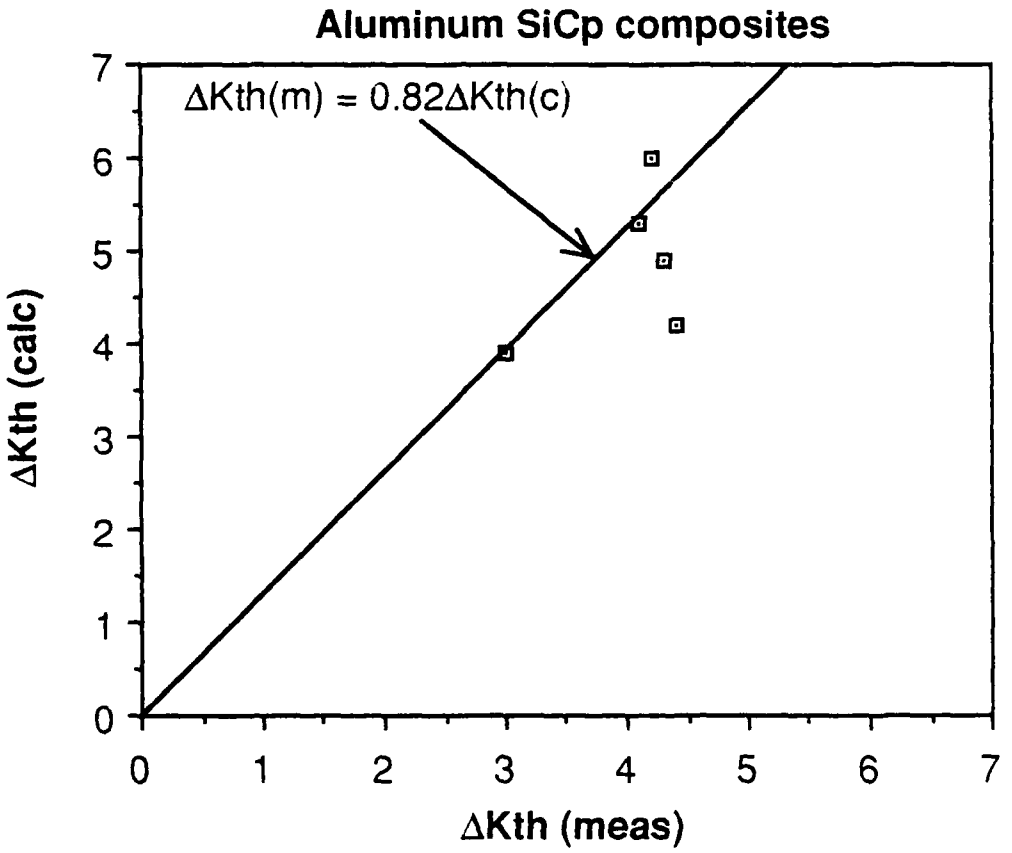


Fig. 6 Comparison between computed and measured values of $\Delta K_{th}$.

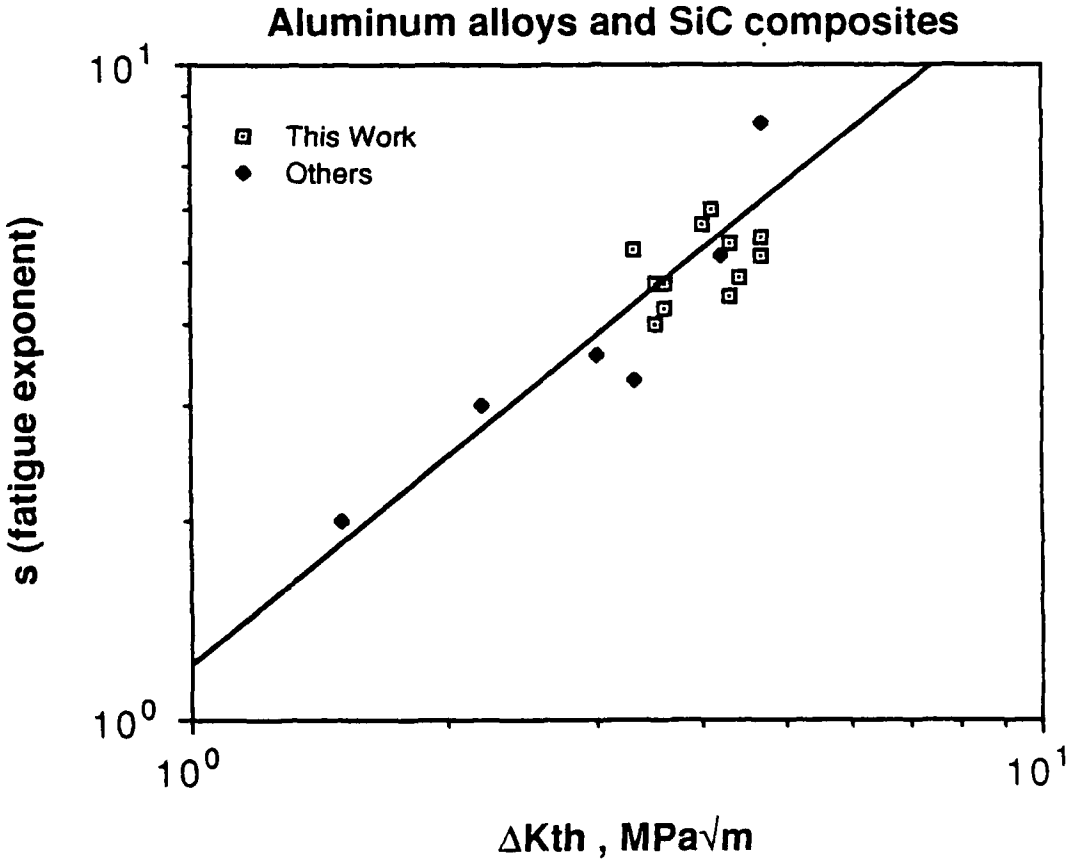


Fig 7 Correlation between paris law exponent s and measured threshold stress intensity factors for the materials studied here (Table 1) and from the work of others (Table 2).

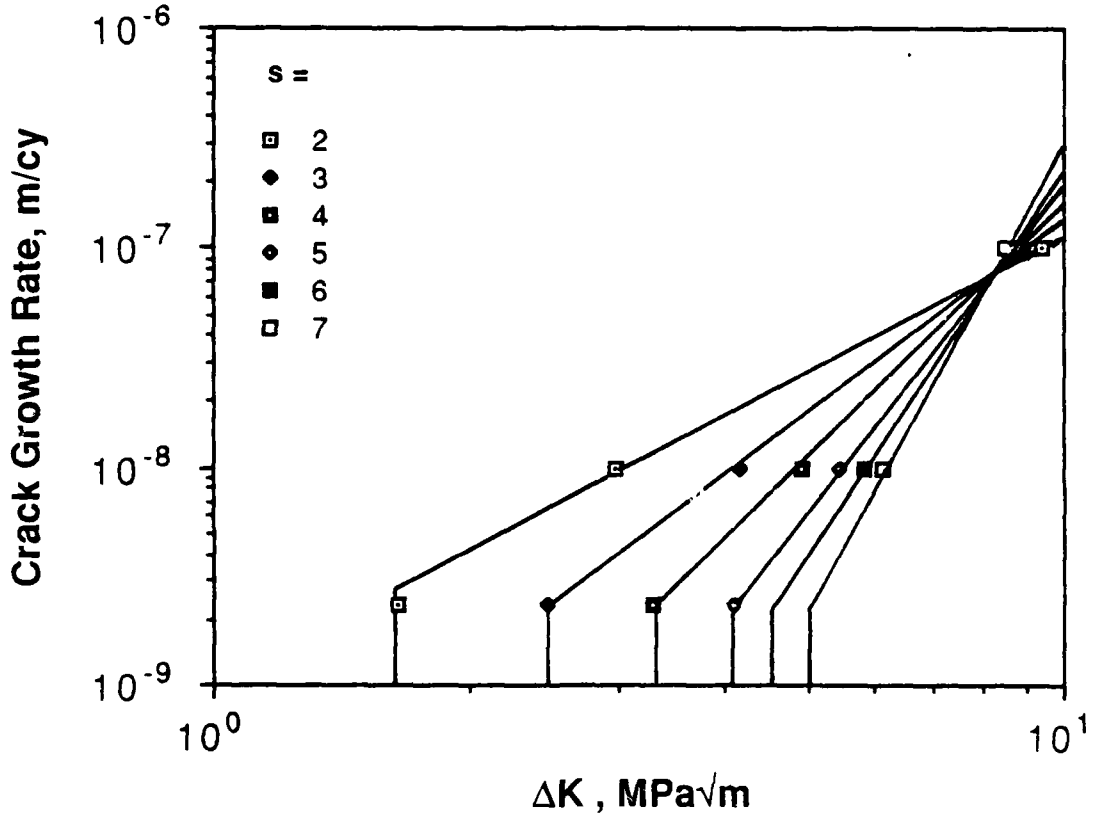


Fig. 8 The family of curves obtained using the empirical correlations found for these materials.

END

DATE

FILMED

DTIC

11-88